Biotechnology for Biofuels

RESEARCH Open Access

Exploring the prospective of weeds (*Cannabis sativa* L., *Parthenium hysterophorus* L.) for biofuel production through nanocatalytic (Co, Ni) gasification

Nadeem Tahir[1], Muhammad Naveed Tahir[2], Mujeeb Alam[1,2], Wang Yi[1*] and Quangou Zhang[1]

Abstract

Background: While keeping in view various aspects of energy demand, quest for the renewable energy sources is utmost. Biomass has shown great potential as green energy source with supply of approximately 14% of world total energy demand, and great source of carbon capture. It is abundant in various forms including agricultural, forestry residues, and unwanted plants (weeds). The rapid growth of weeds not only affects the yield of the crop, but also has strong consequences on the environment. These weeds can grow with minimum nutrient input requirements, have strong ability to grow at various soil and climate environments with high value of cellulose, thus can be valuable source of energy production.

Results: *Parthenium hysterophorus* L. and *Cannabis sativa* L. have been employed for the production of biofuels (biogas, biodiesel and biochar) through nano-catalytic gasification by employing Co and Ni as nanocatalysts. Nanocatalysts were synthesized through well-established sol–gel method. SEM study confirms the spherical morphology of the nanocatalysts with size distribution of 20–50 nm. XRD measurements reveal that fabricated nanocatalysts have pure standard crystal structure without impurity. During gasification of *Cannabis sativa* L., we have extracted the 53.33% of oil, 34.66% of biochar and 12% gas whereas in the case of *Parthenium hysterophorus* L. 44% oil, 38.36% biochar and 17.66% of gas was measured. Electrical conductivity in biochar of *Cannabis sativa* L. and *Parthenium hysterophorus* L. was observed 0.4 dSm−1 and 0.39 dSm−1, respectively.

Conclusion: Present study presents the conversion of unwanted plants *Parthenium hysterophorus* L. and *Cannabis sativa* L. weeds to biofuels. Nanocatalysts help to enhance the conversion of biomass to biofuel due to large surface reactivity. Our findings suggest potential utilization of unwanted plants for biofuel production, which can help to share the burden of energy demand. Biochar produced during gasification can replace chemical fertilizers for soil remediation and to enhance the crop productivity.

Keywords: Weeds, Nano-catalytic gasification, Biofuel, Biomass, Biochar

Background

Economies around the world are facing serious threats because of high energy demands for sustainable economic growth and development. While keeping many challenges in view such as limited resources, high prices of conventional fuels, and environmental pollution, research and development in the renewable energy

*Correspondence: wangyi2543@126.com
[1] Collaborative Innovation Center of Biomass Energy, Henan Agricultural University, Zhengzhou 450002, China
Full list of author information is available at the end of the article

sources is utmost solution [1, 2]. Biomass has shown great potential as green energy source with supply of approximately 14% of world total energy demand, and great source of carbon capture [3]. It is abundant in various forms including agricultural, forestry residues, and unwanted plants (weeds). Feedstocks for second-generation biofuels are already being promoted and include such plant species which can grow fast with minimum nutrient input requirements, have strong ability to grow at various soil and climate environments with high value of cellulose. Most of the work is carried out by adopting biological methods to produce biofuel from various species including *Salix* spp. [4, 5], Eucalyptus spp. [6], Prosopis spp. [7], *Parthenium hysterophorus* L. [8], *Cannabis sativa* L. [9], *Panicum virgatum* L. [10, 11] and Arundo donax L. [12].

The pyrolysis, liquefaction, combustion and gasification are the fundamental thermochemical conversion routes of biomass to biofuel which end up with bioethanol, biodiesel, bio-oil, bio-syngas and biohydrogen. Catalytic gasification has shown great advancement in production of clean energy by converting biomass at low gasification temperatures with high efficiency. The employed catalysts not only help to reduce the reaction time but also help to lower the conversion temperature of biomass to gas of high calorific value [13, 14].

Nanocatalysts have shown great potential to overcome limitations barrier faced by conventional catalysts due to entirely different properties as compared to bulk materials with high surface reactivity. Various nanomaterials have been employed as catalysts including metallic nanoparticles, nanotubes, and nanorods in numerous applications for the production of bioethanol and biodiesel [15, 16]. Catalysts play crucial role in production of biodiesel where transesterification of fats, vegetable oils, and grease (FOG) is carried out through the addition of methanol (or other alcohols). In the standard procedure, the production of biodiesel from biomass is carried out through two steps. During the first step, the biomass is gasified at elevated temperature with resultant byproduct of bio-oil, syngas and biochar which can be good alternative to chemical fertilizers. In the second step, bio-oil is further passed through transesterification to get biodiesel [17]. Biodiesel derived from biomass has been promoted under the aspect of being a "premium" diesel fuel with, for example, a very high cetane number [18].

Addition of catalyst enhances the reaction rate of transesterification process and aids in producing high yields of biodiesel [19]. In relation to substrate phase, they are categorized into homogenous and heterogeneous catalysts [20]. Heterogeneous catalysts have several advantages including ease of recycling by filtration which reduces the operational cost by reusability. Various metallic oxides have been examined for the transesterification process of oils and have emerged as potential heterogeneous catalysts; these include alkali earth metal oxides, transition metal oxides, mixed metal oxides, and supported metal oxides [21]. Veljkovic et al. [22] studied the kinetic of calcined CaO at 500 °C for the transesterification process of biodiesel production from sunflower oil. The reaction was performed using 6:1 mol ratio of methanol to oil, 2 h reaction time, 1 wt% catalyst and 60 °C to achieve 98% of FAME yield. Zhao et al. [23] carried out transesterification of canola oil and methanol using a batch reactor at optimum conditions of 65 °C, with methanol to oil molar ratio of 9:1 and 600 rpm stirring speed. The biodiesel yield over nano-CaO was nearly 81%. Taufiq-Yap et al. [24] showed that by employing metal oxides for catalyzing the transesterification reaction of non-edible *Jatropha curcas* oil to produce biodiesel can be possible route to achieve good results. The catalyst with optimum reaction conditions; 25:1 M ratio of methanol to oil, 3 h, 120 °C, and catalyst loading of 3 wt % for various Ca/Mg atomic ratios show FAME with 70–90% yield range. Safdar Ali et al. [25] showed the production of biogas, biodiesel and biochar from *Carthamus oxyacantha*, *Asphodelus tenuifolius* and *Chenopodium album* through nano-catalytic gasification by employing Ni and Co nanocatalysts, where biodiesel contained 65.47% esters contents. It has been observed that addition of metallic catalysts such as nickel (Ni) and cobalt (Co) significantly enhances the yields of biogas and methane during anaerobic digestion of animal dung [20, 25].

In the present study, we have shown the potential of non-edible resources such as weeds for the production of biofuel (bio-oil and biodiesel) through nanocatalytic gasification process by employing Co and Ni as nanocatalysts. Synthesized nanocatalysts have spherical morphology with standard crystalline structure with size distribution in the range of 20–50 nm. The chemical composition of the extracted biofuel was confirmed through Fourier transform infrared (FTIR) spectroscopy, and gas chromatography/mass spectroscopy (GC–MS) analysis. The conductivity of the byproduct (biochar) highlights the fact that obtained biochar can be used for soil remediation and an alternative to harmful chemical fertilizers which is based on organic components.

Results and discussion

Structural analysis of synthesized Co and Ni nanocatalysts

Surface morphology and crystal structure of the prepared nanocatalysts are shown in Fig. 1. It is clear that Co and Ni nanocatalysts have spherical morphology (Fig. 1a, b) with size distribution of 20-50 nm. The XRD results are consistent with already published work (Mahmood et al. [26] which confirms the correct crystalline phase of the

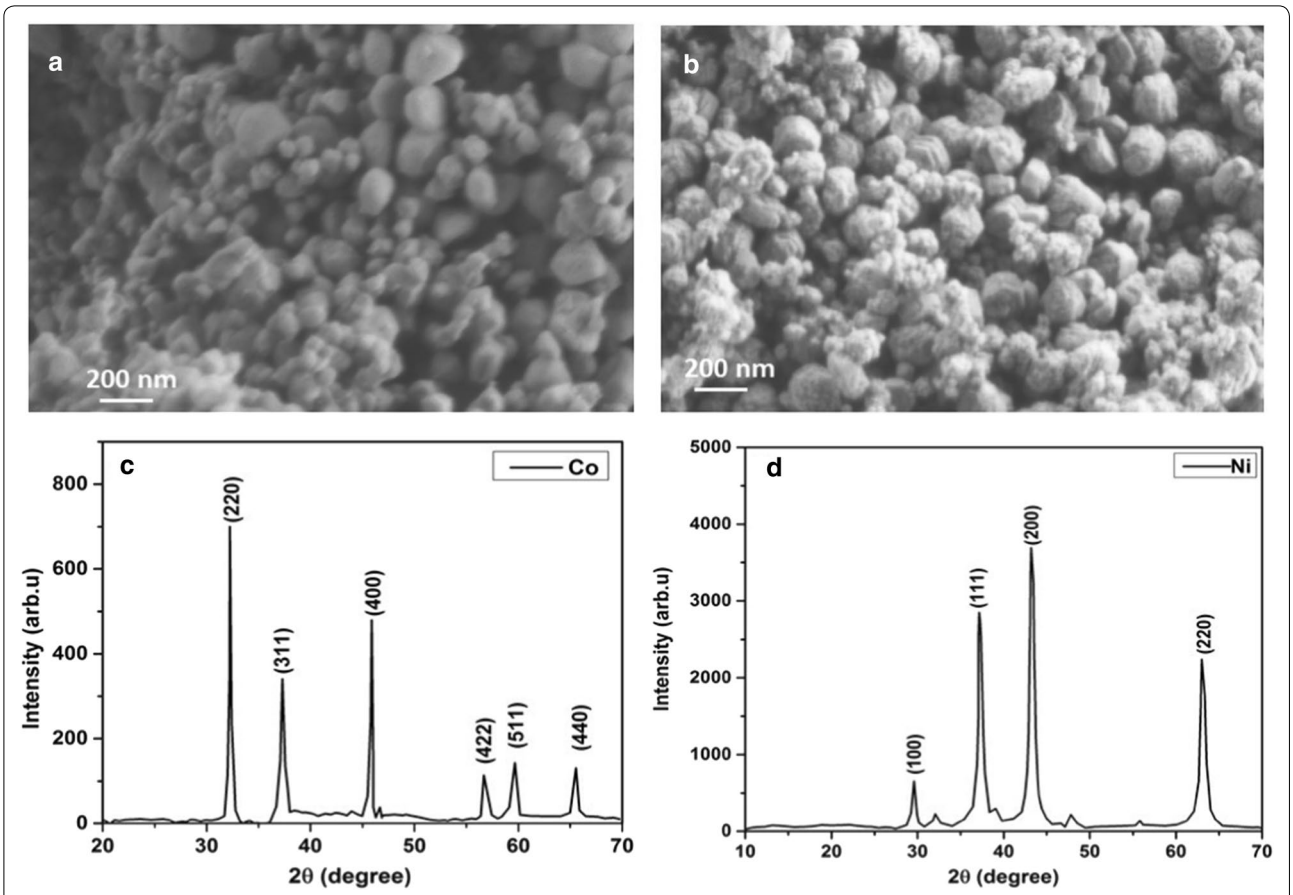

Fig. 1 Structural analysis of nanocatalysts: **a** SEM micrograph of Co nanocatalyst; (**b**) SEM micrograph of Ni nanocatalyst; **c** XRD spectra of Co of nanocatalyst; **d** XRD spectra of Ni nanocatalysts

Co and Ni nanocatalysts. The XRD peaks in cobalt corresponds to the indices (220), (311), (400), (422), (511) and (440) of pure phase centered cube with 2θ angles of 31.8°, 36.9°, 45.5°, 59.4° and 65.3°, respectively [27] (Fig. 1c). Figure 1d illustrates the X-ray diffracted peaks from Ni nanocatalysts which corresponds to indices (100) (111), (200) and (220) with 2θ at 29.4, 37.3, 43.4 and 62.9°, respectively [28, 29].The mean crystal sizes of the particles were calculated through Scherrer formula by calculating full width at half maximum (FWHM) of the major diffracted peaks. The estimated average crystallite size of nanocatalysts were found to be 47.92 nm and 28.85 nm Co and Ni nanocatalysts, respectively.

FTIR analysis of *Cannabis sativa* L. biodiesel and bio-oil

Figure 2a shows the FTIR spectrum of biodiesel from *Cannabis sativa* L. with 9 major observed peaks. The FTIR spectrum indicated that first percentage absorbance peak in biodiesel was at 3339 cm^{-1} while the other was at 696 cm^{-1} whereas in bio-oil the first absorbance peak was observed at 3398 cm^{-1} and last peak was indicated at 612 cm^{-1}. The observed bands between 3000 and 3700 cm^{-1} and 2700–3000 cm^{-1} show O–H and C–H bonds, respectively [30]. The observed peaks around 3398 cm^{-1}, and two around 2883 cm^{-1} and 2826 cm^{-1} were observed in CBO while in CBD 3339 cm^{-1} which express the O–H stretching bonds in phenolic and alcoholic compounds. Observed bands around 2944 cm^{-1} and 2833 cm^{-1} highlight the symmetric and asymmetric stretching vibrational bands of C–H alkanes groups, respectively. In general, the broad spectrum band around 3700–3000 cm^{-1} express the OH or NH stretching vibrational band in materials with cellulose or proteins, whereas weak bands around 2924 and 2850 cm^{-1} represent CH_2 asymmetric and symmetric stretching band, respectively [31]. It is noticed that pronounced absorption bands around 1710 cm^{-1}, and 1712 cm in CBO and CBD are assigned to C=O stretch bond and suggest the presence of fatty acids in samples. The observed band around 1750–1700 cm^{-1} shows the presence of ester carbonyl group in stretching mode [32]. In CBD, the observed peaks at 1409 cm^{-1} 1515 cm^{-1} and

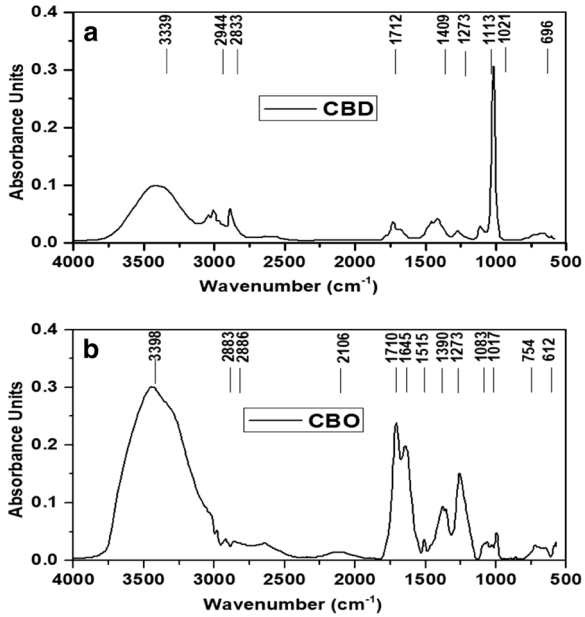

Fig. 2 FTIR analysis of biodiesel and bio-oil: **a** Cannabis sativa L. biodiesel (CBD); **b** Cannabis sativa L. bio-oil (CBO)

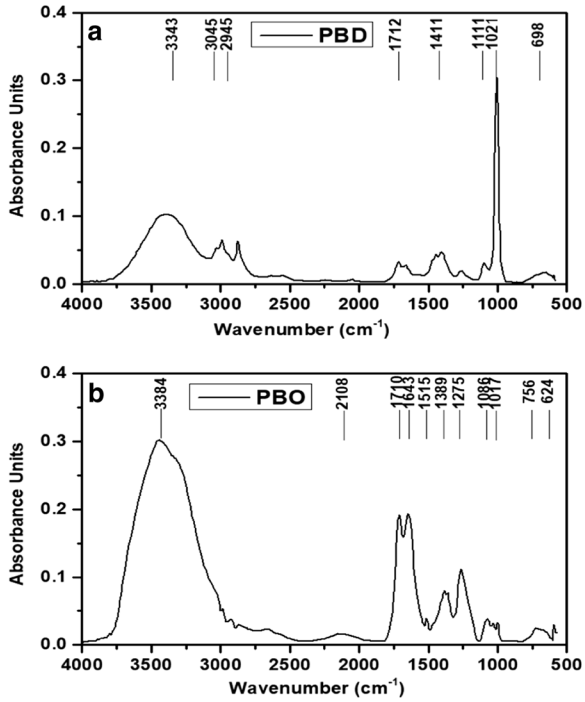

Fig. 3 FTIR analysis of biodiesel and bio-oil: **a** *Parthenium hysterophorus* L. biodiesel (PBD); **b** *Parthenium hysterophorus* L. bio-oil (PBO)

1390 cm^{-1} can be assigned to aromatic compounds from N–H bending mode and methyl (CH_3) bonds. Furthermore, the intensity of 1515 cm^{-1} in CBD is substantially reduced which suggest the removal of lignin and hemicelluloses after transesterification of bio-oil. The observed bands around 1280 and 1000 cm^{-1} suggest the possible existence of acids, phenols or alcohols in the samples due to C–O vibrations [33].

FTIR analysis of *Parthenium hysterophorus* L. biodiesel and bio-oil

Figure 3a shows the FTIR spectrum of biodiesel from *Parthenium hysterophorus* L. with 8 major bands. The observed peak around 3343 cm^{-1} in both PBD and PBO suggests the O–H stretching bond which can be due to the rapturing of hydrogen bonds in cellulose indicating alcohols, phenols remain unchanged in each of the blend sample which confirms the presence of above functional group in both PBD and PBO. Two peaks around 2945 cm^{-1} and 2833 cm^{-1} in PBD were detected while this band was absent in PBO. The observed peaks around 2924 cm^{-1} and 2853 cm^{-1} suggest the presence of CH_2 and CH_3 groups and related to symmetric and antisymmetric stretching vibrations of C–H, respectively [34]. The observed band in PBD and PBO at wave number around 1712 cm^{-1} confirms the existence of esters group with C=O stretching bond. Methyl esters also show their standard carbonyl absorptions characteristics around absorption band of 1820–1680 cm^{-1} which is absent in conventional diesel fuel [35]. Two peaks around 1643 cm^{-1} and 1515 cm^{-1} were observed in bio-oil, but were not detected in biodiesel. Our results of PBO are in good agreement with the results from Kowthaman and Varadappan [35], which confirms that slight bend in the peak around 1647 cm^{-1} ensures the absorption band of olefins. The absorbance peaks at 1389 cm^{-1} and 1275 cm^{-1} in PBD and 1409 cm^{-1} in PBO indicated alkene C–H rock, C–O stretching and alcohol O–H bending, respectively. The observed peak in PBD and PBO within the frequency band of 1120–1090 cm^{-1} confirms the presence of ester due to the stretching vibration of C–O [36]. Similar results were found during the conversion of Jatropha to biodiesel where bands around 1443, 1096 and 965 cm^{-1} disappeared and new bands were formed around 1430 cm^{-1} and 1194 cm^{-1} [36].

GC–MS analysis of biodiesel and bio-oil from *Cannabis sativa* L.

Tables 1 and 2 summarize the results observed from GC–MS analysis of CBD and CBO showing several different chemical compounds according to their molecular weight, respectively. The color of biodiesel was yellowish and less gas was produced during gasification process. It has been noted that there are 10 and 15 major peaks in CBD and CBO, respectively. We can infer from

Table 1 GC–MS of *Cannabis sativa* L. biodiesel (CBD)

Compound name	Peak position	Molecular weight	Chemical formula
Methyl alcohol	1	32	CH_4O
Ethanol	2	46	C_2H_6O
Trichloromethane	3	118	$CHCL_3$
Trichloromethane	4	118	$CHCL_3$
2-Propanone,1-hydroxy	5	74	$C_3H_6O_2$
Cis-13-Eicosenoic acid, methyl ester	6	324	$C_{21}H_{40}O_2$
Cis-13-Eicosenoic acid, methyl ester	7	324	$C_{21}H_{40}O_2$
Cis-13-Eicosenoic acid, methyl ester	8	324	$C_{21}H_{40}O_2$
Cis-13-Eicosenoic acid, methyl ester	9	324	$C_{21}H_{40}O_2$
Eicosenoic acid, methyl ester	10	324	$C_{21}H_{40}O_2$

Table 2 GC–MS of *Cannabis sativa* L. bio-oil (CBO)

Compound name	Peak position	Molecular weight	Chemical formula
Methyl alcohol	1	32	CH_4O
Ethanol	2	46	C_2H_6O
Ethyl format	3	74	$C_3H_6O_2$
Trichloromethane	4	118	$CHCl_3$
Trichloromethane	5	118	$CHCl_3$
2-Propanone,1-hydroxy	6	74	$C_3H_6O_2$
1-Hydroxy-2-butanone	7	88	$C_4H_8O_2$
Furfural	8	96	$C_5H_4O_2$
Butyrolactone	9	86	$C_4H_6O_2$
Butanoic acid, anhydride	10	158	$C_8H_{14}O_3$
Butyric acid, p-methoxyphenyl ester	11	194	$C_{11}H_{14}O_3$
Phenol, 2,6-dimethoxy	12	154	$C_8H_{10}O_3$
1,2,3-Trimethoxybenzene	13	168	$C_9H_{12}O_3$
Benzene, 1,2,3-trimethoxy-5-methyl-	14	182	$C_{10}H_{14}O_3$
9-Octadecenoic acid 12-hydroxy, methyl ester [z]	15	312	$C_{19}H_{36}O_3$

the reported literature that main components identified in biodiesel are methyl alcohol, ethanol, trichloromethane, 2-propanone,1-hydroxy, cis-13-eicosenoic acid and methyl ester (Table 1). On the other hand, major compounds detected in the bio-oil are summarized in Table 2, which include methyl alcohol, ethanol, ethyl format, tri chloromethane, 2-propanone,1-hydroxy, 1-hydroxy-2-butanone, furfural, butyrolactone, butanoic acid, anhydride, butyric acid, p-methoxyphenyl ester, phenol, 2,6-dimethoxy, 9-Octadecenoic acid 12-hydroxy, methyl ester [z], etc. [37].

GC–MS analysis of biodiesel and bio-oil from *Parthenium hysterophorus* L.

Same procedure was adopted for *Parthenium hysterophorus* L., and results of GC–MS from biodiesel (PBD) and bio-oil (PBO) are summarized in Tables 3 and 4, respectively. The color of the biodiesel was brown yellow liquid with less gas production during gasification process. The extracted compounds by GC–MS are summarized in Tables 3 and 4. The differences in the extracted compounds from biodiesel and bio-oil were due to the difference chemical structure of the biodiesel and bio-oil. The main extracted compounds are identified as methyl alcohol, ethanol, acetic acid, methyl ester, tri chloromethane, 2-propanone,1-hydroxy, cis-13-eicosenoic acid, methyl ester [38, 39].

Analysis of biochar

The biochar yield produced from Cannabis and Parthenium after catalytic gasification is 34.66% and 38.36%, respectively, which shows that biochar yield from *Parthenium hysterophorus* L. is higher as compare to *Cannabis sativa* L. The detailed analysis of the derived biochar is summarized in Table 5.

Table 3 GC–MS analysis of *Parthenium hysterophorus* L. biodiesel (PBD)

Compound name	Peak position	Molecular weight	Chemical formula
Methyl alcohol	1	32	CH_4O
Ethanol	2	46	C_2H_6O
Acetic acid, methyl ester	3	74	$C_3H_6O_2$
Trichloromethane	4	118	$CHCl_3$
2-Propanone,1-hydroxy	5	74	$C_3H_6O_2$
Cis-13-Eicosenoic acid, methyl ester	6	324	$C_{21}H_{40}O_2$
Cis-13-Eicosenoic acid, methyl ester	7	324	$C_{21}H_{40}O_2$
Cis-13-Eicosenoic acid, methyl ester	8	324	$C_{21}H_{40}O_2$
Cis-13-Eicosenoic acid, methyl ester	9	324	$C_{21}H_{40}O_2$
Cis-13-Eicosenoic acid, methyl ester	10	324	$C_{21}H_{40}O_2$

Table 4 GC–MS of *Parthenium hysterophorus* L. bio-oil (PBO)

Compound name	Peak position	Molecular weight	Chemical formula
Trichloromethane	1	118	$CHCl_3$
Trichloromethane	2	118	$CHCl_3$
Acetic acid	3	60	$C_2H_4O_2$
2-Propanone,1-hydroxy	4	74	$C_3H_6O_2$
2-Cyclopenten-1-one, 2-hydroxy-3-methyl	5	112	$C_6H_8O_2$
6-Octadecenoic acid, methyl ester, [z]	6	296	$C_{19}H_{36}O_2$
8-Octadecenoic acid, methyl ester	7	296	$C_{19}H_{36}O_2$
9-Octadecenoic acid, methyl ester, [e]	8	296	$C_{19}H_{36}O_2$
Methyl stearate	9	298	$C_{19}H_{38}O_2$
Methyl stearate	10	298	$C_{19}H_{38}O_2$
Octadec-9-enoic acid	12	282	$C_{18}H_{34}O_2$
Phenol, 2,6-dimethoxy	12	154	$C_8H_{10}O_3$
n-Propyl 9,12-ocatdecadienoate	13	322	$C_{21}H_{38}O_2$
Ethyl oleate	14	310	$C_{20}H_{38}O_2$
Ethyl oleate	15	310	$C_{20}H_{38}O_2$

Table 5 Analysis of biochar

Biochar	Yield%	Organic matter%	Total organic carbon%	pH	EC (dS m^{-1})
Cannabis sativa L. biochar	34.66	61.75	35.82	5.3	0.4
Parthenium hysterophorus L. biochar	38.36	56.03	32.5	5.5	0.39

Total organic carbon and organic matter content

The organic matter and total organic carbon compositions of biochars were determined. The total organic carbon content in *Cannabis sativa* L. was found to be 35.82%, which was higher as compare to *Parthenium hysterophorus* L. (32.5%). It is a well-known fact that high contents of carbon in biochar can lead to enhancing plant regeneration, crop production and soil health [40, 41]. In the present study, the obtained biochar from *Cannabis sativa* L. showed higher organic contents which is 61.75% in comparison to 56.03% from *Parthenium hysterophorus* L.

pH

The pH values of the biochar indicated the least difference and showed acidic nature. It is reported that increase in temperature can increase the pH of biochars which could be due to presence of non-gasified inorganic elements in the original feedstocks [42]. In the present study, pH of 5.3 and 5.5 were recorded in the biochar of *Cannabis sativa* L. and in *Parthenium hysterophorus* L., respectively.

Kumar et al. [43] stated that the electrical conductivity (EC) and soil pH increased significantly with *Parthenium hysterophorus* L. biochar addition, but in our study, the *Parthenium hysterophorus* L. showed low pH.

Electrical conductivity (EC)

Electrical conductivity of the soil is an important factor which highlights the presence of nutrients in the soil. Higher value of electrical conductivity leads to increase in negative charges sites, which could eventually effect the plant growth. In standard method of measurement, soil salinity indicates the ability of aqueous solution to pass current. It is very important to study the value of EC of derived biochars before the implementation to limit the deposition of salt. In our study, the electrical conductivity of 0.4 dSm^{-1} and 0.39 dSm^{-1} from biochar of *Cannabis sativa* L. and *Parthenium hysterophorus* L. has been observed, respectively, which is much lower than the saline threshold of 4 dSm^{-1} [44, 45]. Our findings suggests that derived biochar from *Cannabis sativa L* can be potential candidate which can encourage farmers to employ biochar instead chemical fertilizers which have serious concerns to environment.

Reusability of catalyst

The main advantage of heterogenous catalyst is its reusability as it can be easily separated from the reaction mixture. Reusability of catalysts after transesterification reaction of CBO and PBO into biodiesel was tested up to 6 cycles. At the end of each experiment, the catalysts were filtered and stirred in ethanol for 30 min to remove possible traces of polar and non-polar components present on the surface of the catalysts. The catalysts were dried at 60 °C in an oven under Ar gas flow for 12 h. It can be seen from Fig. 4 that these catalysts have good reusability up to 4 cycle, whereas efficiency dropped sharply to 65% and 40% in the 5th and 6th cycle, respectively. The decrease in catalytic activity with each cycle could due to the blockage of catalyst active sites because of the deposition of glycerol, free fatty acids and leaching of $–SO_3H$ from biochar [46–48].

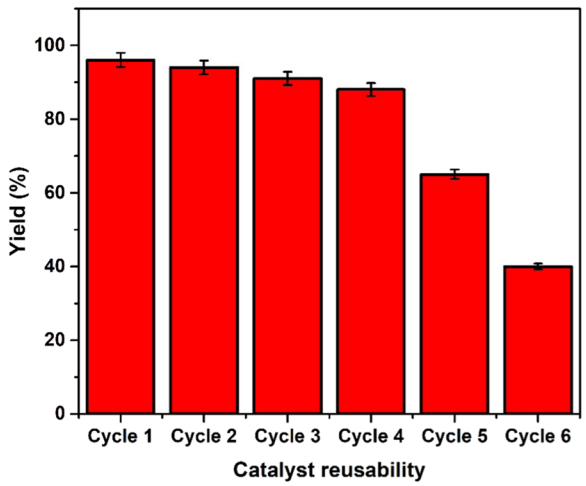

Fig. 4 Reusability of the catalyst

Conclusion

We have shown the potential of biofuel production from *Cannabis sativa* L. and *Parthenium hysterophorus L* weeds through nanocatalytic gasification which grows vastly in monsoon season. Due to high surface-to-volume ratio of nanocatalysts, the conversion of biomass to biofuel was achieved at low temperature. The results showed that efficiency of biodiesel production from *Cannabis sativa* L. is 53% which is higher as compare to available literature. The total organic carbon contents in biochar from *Cannabis sativa* L. and *Parthenium hysterophorus L* were found to be 35.82% and 32.5%, respectively. Low value of electrical conductivity of the biochar suggest that it can be implemented to reduce farmer dependence of chemical fertilizers which have serious threats to our environment.

Materials and methods

The biomass samples of weeds namely industrial hemp (*Cannabis sativa* L.) and carrot grass (*Parthenium hysterophorus* L.) were collected from the research field area of PMAS-Arid Agriculture University Rawalpindi, Pakistan. All the samples were naturally dried and later crushed by mechanical grinder (MF 10 IKA, Werke, Germany) in submicron particle size by passing through sieve of 500µm. All the chemicals of analytical reagent grade were purchased from Sigma Aldrich. To synthesize nanocatalysts of Co and Ni, we slightly modified the procedure described in Mahmood et al. [26]. In a particular experiment, 0.5 M solution of 1, 10 phenanthroline and 0.5 M solution of cobalt chloride ($CoCl_2.6H_2O$) were individually prepared in 1-propanol. In the following step, 1,10 phenanthroline solution was added slowly into the solution of cobalt chloride with continuous stirring at 45 °C. The resultant pink precipitates were filtered and washed several times with 1-propanol to minimize the un-reacted salts. Prior to anneal samples were dried in the oven at 60 °C for 12 h to remove the moisture contents. Synthesized samples were annealed in tube furnace at temperature of 500 °C for 8 h under the flow of Ar to get the desire crystalline phase. Similar procedure was adopted to synthesize Ni nanocatalysts.

Microstructures of the synthesized Co and Ni nanocatalysts were studied by JSM-7500 scanning electron microscope (SEM) whereas crystalline structure was

studied by X-ray diffractometer from PANalytical, Netherlands, (Model 3040/60 X-pert PRO).

FTIR analysis is non-destructive and the most widely employed experimental tool to analyze the chemical structure of the resulted product by studying functional groups and the bands. FTIR analysis of the transesterified biodiesel and the bio-oil obtained from studied samples was carried out by Thermo-Nicolet Nexus 670 Spectrophotometer. 1 mg of investigated sample was mixed with 100 mg of KBr to scan in the range 550 to 4000 $cm^{-}1$ with resolution of 1 $cm^{-}1$ [49]. All the collected gaseous samples were characterized by GC–MS Hewlett-Packard [Palo Alto, A] 5890 series II gas chromatograph with Hewlett-Packard 5972 mass selective detector by following the procedure described previously [50]. Transesterification was performed according to the methodologies adopted by Mahmood et al. [51]. The biochar was analyzed for organic matter content, total organic carbon content, pH and electrical conductivity (EC) by employing Multimeter (CRISON MM 40ₚ) by dissolving 1 g of biochar into 5 ml distilled water while shaking at 150 rpm for 30 min.

Nano-catalytic gasification

In particular, experiment 100 g of respective dried biomass (*cannabis sativa* L. *and Parthenium hysterophorus* L.) was separately mixed with 1 g of nanocatalysts (Co (0.5 g) and Ni (0.5 g)) with ratio of 50/50 and gasified in a round bottom flask at 300 °C. The biochar was settled down at the of bottom flask whereas the gas was collected in gas collecting bag outside the gasifier. Furthermore, bio-oil was condensed to collect in a measuring cylinder whereas moisture contents were removed by dehydrating around 90 °C. Samples of produced gas were examined through gas chromatography–mass spectrometry. The quantity of hydrocarbon and syngas was measured. During gasification of Cannabis sativa L., we have extracted the 53.33% of oil, 34.66% of biochar and 12% gas, whereas in the case of Parthenium hysterophorus L. 44% oil, 38.36% biochar and 17.66% of gas was measured.

Nano-catalytic transesterification

Methanol of 300 ml was mixed with 0.2 g from Ni and Co nanocatalysts with ratio of 50/50 (0.1 g Ni, and 0.1 g Co). The nanocatalyst enhanced the esterification of methanol. The solution was continuously stirred and refluxed at 80 °C for 1 h. In the next step, bio-oil samples were mixed and refluxed for 2 h at 80 °C with catalytic alcoholic mixture. The resulting mixture was allowed to settle down. Two layers with upper transparent layer of biodiesel and lower layer of used catalysts and glycerin were established. The quantity of each product was measured. The catalysts recovered by filtration were washed with ethanol to remove organic components for better performance and dried in oven at 60 °C for 12 h under Ar gas flow.

Abbreviations

AAEMs: Alkali and alkaline earth metals; FTIR: Fourier transform infrared spectroscopy; SEM: Scanning electron microscope; XRD: X-ray diffraction; GC–MS: Gas chromatography/mass spectroscopy; CBD: Cannabis biodiesel; PBD: Parthenium biodiesel; CBO: Cannabis bio-oil; PBO: Parthenium bio-oil; Ni: Nickel; Co: Cobalt; EC: Electrical conductivity; NO_x: Nitrous oxide; SO_x: Sulphur oxide; NC: Nano-catalyst.

Acknowledgements

The authors gratefully acknowledged the financial support from Top Notch Talent program, Henan Agricultural University (30500598), State-Sponsored Scholarship Program (NO. 201908410130), and National Natural Science Foundation of China (NO. 51376056, 51576060).

Authors' contributions

NT: designing and performing experiment, writing manuscript, and financial support for the project leading to this publication. MNT: plan of experiment, and proof reading. MA: handling of data and writing manuscript. WY: corresponding author, responsible for ensuring that the descriptions are accurate and agreed by all authors, financial support. QZ: 2nd corresponding author, responsible for ensuring that the descriptions are accurate and acquisition of the financial support for the project leading to this publication. All authors read and approved the final manuscript.

Funding

Top Notch Talent program, Henan Agricultural University (30500598), State-Sponsored Scholarship Program (NO. 201908410130) and National Key Research and Development Program of China (NO. 2018YFE0206600), National Natural Science Foundation of China (NO. 51676065).

Availability of data and materials

Not applicable.

Ethics approval and consent to participate

The studied weeds were locally collected from the research farm of research field area of PMAS-Arid Agriculture University Rawalpindi, Pakistan.

Consent for publication

Not applicable.

Competing interests

We verify that there are no conflicts of interest to present work. We declare that we do not have any commercial or associative interest that may cause conflict of interest in connection with the submitted work.

Author details

[1] Collaborative Innovation Center of Biomass Energy, Henan Agricultural University, Zhengzhou 450002, China. [2] Department of Agronomy, PMAS-Arid Agriculture University Rawalpindi, Rawalpindi 46300, Pakistan.

Received: 17 March 2020 Accepted: 8 August 2020
Published online: 20 August 2020

References

1. Pang S. Advances in thermochemical conversion of woody biomass to energy, fuels and chemicals. Biotechnol Adv. 2019;37:589–97.
2. Mallick D, Mahanta P, Moholkar VS. Synergistic effects in gasification of coal/biomass blends: analysis and review. 2018. p. 473–97. https://doi.org/10.1007/978-981-10-7335-9_19
3. Mamaeva A, Tahmasebi A, Tian L, Yu J. Microwave-assisted catalytic pyrolysis of lignocellulosic biomass for production of phenolic-rich bio-oil. Bioresour Technol. 2016;211:382–9.

4. Fenning T, editor. Challenges and Opportunities for the World's Forests in the 21st Century. Dordrecht: Springer Netherlands; 2014.
5. Cunniff J, Purdy SJ, Barraclough TJP, Castle M, Maddison AL, Jones LE, et al. High yielding biomass genotypes of willow (Salix spp.) show differences in below ground biomass allocation. Biomass Bioenergy. 2015;80:114–27.
6. McIntosh S, Vancov T, Palmer J, Spain M. Ethanol production from Eucalyptus plantation thinnings. Bioresour Technol. 2012;110:264–72.
7. Park SC, Ansley RJ, Mirik M, Maindrault MA. Delivered biomass costs of honey mesquite (*Prosopis glandulosa*) for bioenergy uses in the South Central USA. BioEnergy Res. 2012;5:989–1001. https://doi.org/10.1007/s12155-012-9214-2.
8. Tavva SSMD, Deshpande A, Durbha SR, Palakollu VAR, Goparaju AU, Yechuri VR, et al. Bioethanol production through separate hydrolysis and fermentation of *Parthenium hysterophorus* biomass. Renew Energy. 2016;86:1317–23.
9. Rehman MSU, Rashid N, Saif A, Mahmood T, Han J-I. Potential of bioenergy production from industrial hemp (*Cannabis sativa*): Pakistan perspective. Renew Sustain Energy Rev. 2013;18:154–64.
10. Nelson RS, Stewart CN, Gou J, Holladay S, Gallego-Giraldo L, Flanagan A, et al. Development and use of a switchgrass (*Panicum virgatum* L.) transformation pipeline by the BioEnergy Science Center to evaluate plants for reduced cell wall recalcitrance. Biotechnol Biofuels. 2017;10:309. https://doi.org/10.1186/s13068-017-0991-x.
11. Alexopoulou E, Monti A, Elbersen HW, Zegada-Lizarazu W, Millioni D, Scordia D, et al. Switchgrass. Perenn grasses bioenergy bioprod. New Jersey: Elsevier; 2018. p. 61–105.
12. Forte A, Zucaro A, Faugno S, Basosi R, Fierro A. Carbon footprint and fossil energy consumption of bio-ethanol fuel production from *Arundo donax* L. crops on marginal lands of Southern Italy. Energy. 2018;150:222–35.
13. Ong HC, Chen W-H, Farooq A, Gan YY, Lee KT, Ashokkumar V. Catalytic thermochemical conversion of biomass for biofuel production: a comprehensive review. Renew Sustain Energy Rev. 2019;113:109266.
14. Bhavanam A, Sastry RC. Biomass gasification processes in downdraft fixed bed reactors: a review. Int J Chem Eng Appl. 2011;2:425–33.
15. Srivastava N, Srivastava M, Pandey H, Mishra PK, Ramteke PW, editors. Green Nanotechnology for Biofuel Production. Cham: Springer International Publishing; 2018. http://link.springer.com/10.1007/978-3-319-75052-1.
16. Rai M, da Silva SS, editors. Nanotechnology for Bioenergy and Biofuel Production. Cham: Springer International Publishing; 2017. http://link.springer.com/10.1007/978-3-319-45459-7.
17. Dahiya A, editor. Bioenergy. 2nd Edition. New Jersey: Elsevier; 2020. https://linkinghub.elsevier.com/retrieve/pii/C20170010674.
18. Knothe G. Biodiesel and renewable diesel: a comparison. Prog Energy Combust Sci. 2010;36:364–73.
19. Akia M, Yazdani F, Motaee E, Han D, Arandiyan H. A review on conversion of biomass to biofuel by nanocatalysts. Biofuel Res J. 2014;01:16–25. http://www.biofueljournal.com/pdf_4747_5a92b5c3cb64907a765d44d1e7a57be5.html.
20. Abdelsalam E, Samer M, Attia YA, Abdel-Hadi MA, Hassan HE, Badr Y. Comparison of nanoparticles effects on biogas and methane production from anaerobic digestion of cattle dung slurry. Renew Energy. 2016;87:592–8.
21. Saoud K. Nanocatalyst for biofuel production: a review. Cham: Springer; 2018. p. 39–62.
22. Veljković VB, Stamenković OS, Todorović ZB, Lazić ML, Skala DU. Kinetics of sunflower oil methanolysis catalyzed by calcium oxide. Fuel. 2009;88:1554–62.
23. Zhao L, Qiu Z, Stagg-Williams SM. Transesterification of canola oil catalyzed by nanopowder calcium oxide. Fuel Process Technol. 2013;114:154–62.
24. Taufiq-Yap YH, Lee HV, Yunus R, Juan JC. Transesterification of non-edible Jatropha curcas oil to biodiesel using binary Ca–Mg mixed oxide catalyst: effect of stoichiometric composition. Chem Eng J. 2011;178:342–7.
25. Ali S, Shafique O, Mahmood S, Mahmood T, Khan BA, Ahmad I. Biofuels production from weed biomass using nanocatalyst technology. Biomass Bioenergy. 2020;139:105595.
26. Mahmood T, Hussain ST, Malik SA. New nanomaterial and process for the production of biofuel from metal hyper accumulator water hyacinth. African J Biotechnol. 2010;9:2381–91.
27. Nassar MY, Mohamed TY, Ahmed IS. One-pot solvothermal synthesis of novel cobalt salicylaldimine–urea complexes: a new approach to Co3O4 nanoparticles. J Mol Struct. 2013;1050:81–7.
28. Prabhu YT, Rao KV, Kumari BS, Sai VS, Pavani T. Nickel and nickel oxide nanocrystals selectively grafting on multiwalled carbon nanotubes. Nano Converg. 2015;2:2.
29. Macdonald T, Xu J, Elmas S, Mange Y, Skinner W, Xu H, et al. NiO nanofibers as a candidate for a nanophotocathode. Nanomaterials. 2014;4:256–66.
30. Mohamed Shameer P, Ramesh K. FTIR assessment and investigation of synthetic antioxidant on the fuel stability of *Calophyllum inophyllum* biodiesel. Fuel. 2017;209:411–6.
31. Liu Y, He Z, Shankle M, Tewolde H. Compositional features of cotton plant biomass fractions characterized by attenuated total reflection Fourier transform infrared spectroscopy. Ind Crops Prod. 2016;79:283–6.
32. Al-Samaraae RR, Atabani AE, Uguz G, Kumar G, Arpa O, Ayanoglu A, et al. Perspective of safflower (*Carthamus tinctorius*) as a potential biodiesel feedstock in Turkey: characterization, engine performance and emissions analyses of butanol–biodiesel–diesel blends. Biofuels. 2017. https://doi.org/10.1080/17597269.2017.1398956.
33. Nazari L, Yuan Z, Souzanchi S, Ray MB, Xu C. Hydrothermal liquefaction of woody biomass in hot-compressed water: catalyst screening and comprehensive characterization of bio-crude oils. Fuel. 2015;162:74–83.
34. Ali CH, Asif AH, Iqbal T, Qureshi AS, Kazmi MA, Yasin S, et al. Improved transesterification of waste cooking oil into biodiesel using calcined goat bone as a catalyst. Energy Sources Part A Recover Util Environ Eff. 2018;40:1076–83. https://doi.org/10.1080/15567036.2018.1469691.
35. Kowthaman CN, Varadappan AMS. Synthesis, characterization, and optimization of *Schizochytrium* biodiesel production using Na+-doped nanohydroxyapatite. Int J Energy Res. 2019;43:3182–200.
36. Nisar J, Razaq R, Farooq M, Iqbal M, Khan RA, Sayed M, et al. Enhanced biodiesel production from Jatropha oil using calcined waste animal bones as catalyst. Renew Energy. 2017;101:111–9.
37. Ullah K, Ahmad M, Sultana S, Teong LK, Sharma VK, Abdullah AZ, et al. Experimental analysis of di-functional magnetic oxide catalyst and its performance in the hemp plant biodiesel production. Appl Energy. 2014;113:660–9.
38. Patil PD, Gude VG, Mannarswamy A, Cooke P, Munson-McGee S, Nirmalakhandan N, et al. Optimization of microwave-assisted transesterification of dry algal biomass using response surface methodology. Bioresour Technol. 2011;102:1399–405.
39. Akay G, Jordan CA, Mohamed AH. Syngas cleaning with nano-structured micro-porous ion exchange polymers in biomass gasification using a novel downdraft gasifier. J Energy Chem. 2013;22:426–35.
40. Lehmann J. A handful of carbon. Nature. 2007;447:143–4. http://www.nature.com/articles/447143a.
41. Ramlow M, Rhoades CC, Cotrufo MF. Promoting revegetation and soil carbon sequestration on decommissioned forest roads in Colorado, USA: a comparative assessment of organic soil amendments. For Ecol Manage. 2018;427:230–41.
42. Novak J, Lima I, Xing B, Gaskin J, Steiner C, Das K, et al. Characterization of designer biochar produced at different temperatures and their effects on a loamy sand. Ann Environ Sci. 2009;3:195–206.
43. Kumar S, Masto RE, Ram LC, Sarkar P, George J, Selvi VA. Biochar preparation from *Parthenium hysterophorus* and its potential use in soil application. Ecol Eng. 2013;55:67–72.
44. Munshower FF. Practical handbook of disturbed land revegetation. Boca Raton: CRC Press; 2018.
45. Johannes Lehmann SJ, editor. Biochar for environmental management: science and technology. Earthscan Publications Ltd.; 1 edition (March 2009); 2009.
46. Bhatia SK, Gurav R, Choi T-R, Kim HJ, Yang S-Y, Song H-S, et al. Conversion of waste cooking oil into biodiesel using heterogenous catalyst derived from cork biochar. Bioresour Technol. 2020;302:122872.
47. Gardy J, Rehan M, Hassanpour A, Lai X, Nizami A-S. Advances in nanocatalysts based biodiesel production from non-food feedstocks. J Environ Manage. 2019;249:109316.
48. Sandouqa A, Al-Hamamre Z, Asfar J. Preparation and performance investigation of a lignin-based solid acid catalyst manufactured from olive cake for biodiesel production. Renew Energy. 2019;132:667–82.

49. Yi W, Nadeem F, Xu G, Zhang Q, Joshee N, Tahir N. Modifying crystallinity, and thermo-optical characteristics of *Paulownia* biomass through ultrafine grinding and evaluation of biohydrogen production potential. J Clean Prod. 2020;269:122386.
50. Tsukatani H, Tobiishi K, Imasaka T. Simple and sensitive determination of 2,4-Xylenol in surface water samples from river and sea by gas chromatography–mass spectrometry. Bull Environ Contam Toxicol. 2009;82:153–7. https://doi.org/10.1007/s00128-008-9594-3.
51. Mahmood T, Malik M, Bano A, Umer J, Shaheen A. Nanocatalytic conversion of waste palm oil grade III and poplar plant's wood sawdust into fuel. Innov Energy Res. 2017;6:170–7.

Publisher's Note